

# Effects of Static Magnetic Islands on Interchange mode in Straight Heliotron Configuration

Kinya SAITO<sup>1)</sup>, Katsuji ICHIGUCHI<sup>1,2)</sup> and Nobuyoshi OHYABU<sup>1,2)</sup>

<sup>1)</sup>The Graduate University for Advanced Studies, Toki 509-5292, Japan

<sup>2)</sup>National Institute for Fusion Science, Toki 509-5292, Japan

The interaction between resistive interchange mode with single helicity and static islands due to an external perturbed field is numerically studied in a straight heliotron configuration based on the reduced MHD equations. Especially, the dependence of the island width in the saturation state of the interchange mode on the static island width or the external field magnitude is focused. The dependence is different between the large and small static island cases. In the large static island case, the saturated island width increases as the static island width. In this case, the interchange mode reduces the island width. On the other hand, in the small static island case, the saturated width has an oscillatory tendency with respect to the static island width.

Keywords: magnetic island, resistive interchange mode

## 1. Introduction

In the magnetic confinement of the fusion plasma, a configuration with nested surfaces is the most favorable. However, error magnetic field originated from such as misalignment of the field coils and the terrestrial magnetism induces static magnetic islands. The static islands have a possibility to degrade the plasma confinement substantially. Particularly, the heliotron configuration is easily affected by the static islands because all of the confinement magnetic field is generated by the outer coils. In the Large Helical Device (LHD), which is a typical heliotron device, the Local Island Divertor coils are installed in the system to control the static islands with  $(m, n) = (1, 1)$  actively and investigate the effects on the global confinement[1], where  $m$  and  $n$  are the poloidal and toroidal mode numbers, respectively.

On the other hand, the interchange mode is a crucial MHD mode in the heliotron configurations. A lot of theoretical analyses have been done for the behavior in the nested surface configurations. However, only a few works treated the behavior of the interchange mode in the existence of the static islands. Therefore, comprehensive study about the direct interaction between the interchange mode and the static islands has not been carried out. Thus, the interaction between the static magnetic island and the dynamics of the interchange mode is numerically analyzed in the present work. Particularly, the island width in the saturation state of the interchange mode is focused. To investigate the basic mechanism, we employ a straight heliotron configuration corresponding to the LHD.

## 2. Basic Equations and Incorporation of Static Magnetic islands

Since the nonlinear treatment is inevitable for the study of the magnetic islands, we utilize the NORM

code[2]. This code solves the nonlinear reduced MHD equations for the poloidal magnetic flux  $\Psi$ , the stream function  $\Phi$  and the plasma pressure  $P$ . In the straight heliotron configurations, the equations in the cylindrical coordinates  $(r, \theta, z)$  are given by

$$\frac{\partial}{\partial t} \left( \frac{\tilde{\Psi}}{R_0} \right) = -\frac{1}{\mu_0} \mathbf{B} \cdot \nabla \tilde{\Phi} + \eta \tilde{J}_z \quad (1)$$

$$\rho \frac{d}{dt} \tilde{U} = -(\mathbf{B} \cdot \nabla \tilde{J}_z + \tilde{\mathbf{B}} \cdot \nabla J_z) + \nabla \Omega_{eq} \times \nabla \tilde{P} \cdot \hat{z} + \nu \nabla_{\perp}^2 \tilde{U} \quad (2)$$

and

$$\frac{dP}{dt} = \kappa_{\perp} \nabla \cdot \nabla_{\perp} \tilde{P} + \kappa_{\parallel} \frac{\mathbf{B}}{B_0} \cdot \nabla \left( \frac{\mathbf{B}}{B_0} \cdot \nabla \tilde{P} \right), \quad (3)$$

where the subscript 'eq' refers to the equilibrium quantity and the tilde denotes the perturbed quantity. The factors of  $\rho$  and  $\mu_0$  are the mass density and the vacuum permeability, respectively. The magnetic differential operator and the convective time derivative are given by

$$\mathbf{B} \cdot \nabla = B_0 \frac{\partial}{\partial z} + \hat{z} \times \nabla \left\{ \frac{1}{R_0} (\Psi_{eq} + \tilde{\Psi}) \right\} \cdot \nabla \quad (4)$$

and

$$\frac{d}{dt} = \frac{\partial}{\partial t} + \tilde{\mathbf{v}}_{\perp} \cdot \nabla, \quad (5)$$

respectively, where  $\tilde{\mathbf{v}}_{\perp} = \nabla \tilde{\Phi} \times \hat{z}$ . The operator  $\nabla_{\perp}$  is defined as  $\nabla_{\perp} = \nabla - \hat{z}(\partial/\partial z)$  and  $\hat{z}$  is the unit vector in the  $z$  direction. The vorticity  $\tilde{U}$  and the current density  $\tilde{J}_z$  are expressed by  $\tilde{U} = \nabla_{\perp}^2 \tilde{\Phi}$ ,  $\tilde{J}_z = \nabla_{\perp}^2 (\tilde{\Psi}/R_0)$ , respectively. The average field line curvature  $\Omega_{eq}$  is given by

$$\Omega_{eq} = \frac{1}{4\pi^2} \int_0^{2\pi} \int_0^{2\pi} d\theta d\zeta \left( \frac{R}{R_0} \right)^2 \left( 1 + \frac{|\mathbf{B}_{eq} - \overline{\mathbf{B}_{eq}}|^2}{B_0^2} \right). \quad (6)$$

The viscosity and the perpendicular and parallel heat conductivity are introduced with the coefficients of  $\nu$ ,  $\kappa_{\perp}$  and

author's e-mail: saito.kinya@nifs.ac.jp

$\kappa_{//}$ , respectively. The resistivity  $\eta$  is also introduced, which is measured by the magnetic Reynolds number  $S$  hereafter.

The effects of the static island are incorporated by assuming the existence of an external poloidal magnetic flux perturbation at the plasma boundary[3]. The poloidal flux corresponding to the  $(m, n)$  magnetic islands in vacuum configuration is given by the solution of the current-free equation,

$$\nabla_{\perp}^2 \tilde{\Psi} = 0 \quad (7)$$

with the boundary condition,

$$\tilde{\Psi}_{(r=1)} = \Psi_b \cos(m\theta - n\frac{z}{R_0}). \quad (8)$$

The size of the static magnetic islands is controlled by changing the value of  $\Psi_b$ . Here,  $\Psi_b$  corresponds to the magnitude of the external perturbed magnetic field. We use the solution of Eq.(7) as the initial condition of  $\tilde{\Psi}$  for the nonlinear calculation. By following the time evolution of the interchange mode under the boundary condition (8), we can investigate the effects of the static island on the dynamics of the mode. In the present work, the magnetic island  $(m, n) = (1, 1)$  is examined.

We study the interaction between the static islands and the interchange mode with  $(m, n) = (1, 1)$ . For this purpose, we assume that the perturbations have a single helicity of  $n/m = 1$  as follows:

$$\tilde{\Psi}(r, \theta, z) = \sum_{n=0, m=n}^N \Psi_{m,n}(r) \cos(m\theta - n\frac{z}{R_0}) \quad (9)$$

$$\tilde{\Phi}(r, \theta, z) = \sum_{n=0, m=n}^N \Phi_{m,n}(r) \sin(m\theta - n\frac{z}{R_0}) \quad (10)$$

$$\tilde{P}(r, \theta, z) = \sum_{n=0, m=n}^N P_{m,n}(r) \cos(m\theta - n\frac{z}{R_0}), \quad (11)$$

where  $N = 30$  is employed in the present calculation. The magnetic energy of the perturbation is defined as  $E_M = \sum_n E_M^n$  and  $E_M^n = \frac{1}{2} \int |\nabla_{\perp} \Psi_{nn} \cos(n\theta - n\frac{z}{R_0})|^2 dV$ .

### 3. Equilibrium and Linear Stability

We examine a straight heliotron equilibrium corresponding to the LHD configuration with the vacuum magnetic axis located at 3.6m. The equilibrium is obtained by utilizing the cylindrical part of a three-dimensional equilibrium, which is calculated with the VMEC code[4] under the no net current and the free boundary conditions. We assume the pressure profile of the  $P = P_0(1 - r^4)^2$  with the beta value at the axis of  $\beta_0 = 4\%$ . Figure 1 shows the profiles of the pressure and rotational transform  $\iota$ . The rational surface of  $\iota = 1$  is located at  $r = 0.85$  with substantial pressure gradient.

In order to enhance the effect of the interchange mode, we use a large resistivity of  $S = 10^4$ . We also choose the dissipation parameters of  $\nu$ ,  $\kappa_{\perp}$  and  $\kappa_{//}$  so that

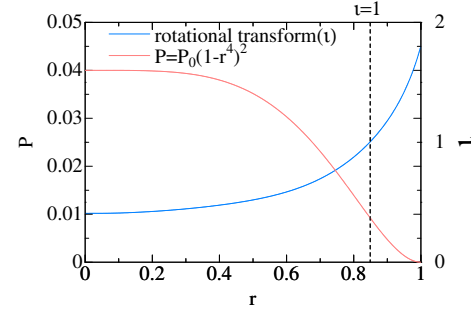


Fig. 1 Profiles of pressure and rotational transform.

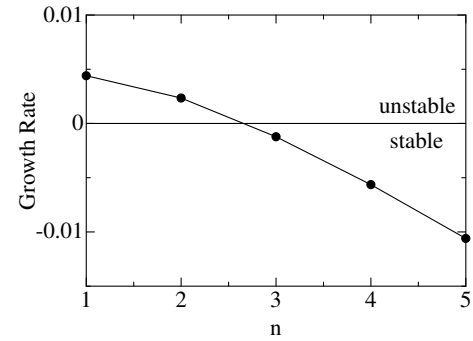


Fig. 2 Linear growth rates of the interchange mode with  $\Psi_b = 0$  versus toroidal mode number  $n$ .

the  $n = 1$  mode should be dominant. Figure 2 shows the linear growth rates for these parameters. The growth rate decreases as the toroidal mode number  $n$ . Only the  $n = 1$  and  $n = 2$  modes are linearly unstable. The growth rate of the  $n = 1$  mode is almost twice of that of the  $n = 2$  mode.

### 4. Development of Magnetic Islands due to Nonlinear Dynamics of Resistive Interchange Mode

We examine the development of the magnetic islands in the nonlinear evolution of the resistive interchange mode discussed in Sec.3. Figure 3 shows the dependence of both widths of the initial static islands at  $t = 0\tau_A(w_i)$  and the islands in the saturation state at  $t = 14,000\tau_A(w_s)$  on the external poloidal flux  $\Psi_b$ . Positive and negative values correspond to the magnetic islands with the X-points located at  $\theta = 0$  and  $\theta = \pi$  in the  $z = 0$  poloidal cross section, respectively. The width of initial island  $w_i$  is a monotonous function of  $\Psi_b$ . However, the tendency of the island width in the saturation state  $w_s$  varies depending on  $\Psi_b$ .

At first, we look at the case of  $w_i = 0$  ( $\Psi_b = 0$ ) as the reference of the case without the static islands. In this case, a typical evolution of the resistive interchange mode is obtained. Figure 4 shows the time evolution of the magnetic energy. There exists a stationary saturation region after the linear growth of the mode. The  $(m, n) = (1, 1)$  mode is dominant in the whole region as expected in Sec.3. Figure 5 shows the contour of the helical magnetic flux in the

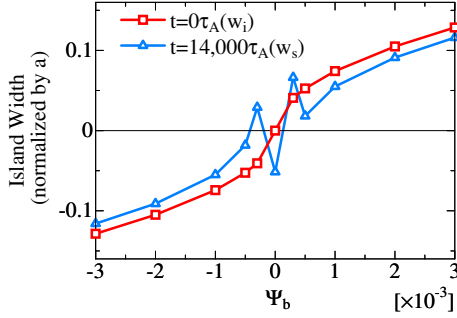


Fig. 3 Dependence of island width in the initial state( $w_i$ ) and the saturation state( $w_s$ ) on  $\Psi_b$ . The width is normalized by the minor radius.

saturation state at  $t = 14,000\tau_A$ , which is defined as

$$\Psi_h(r, \theta, z) = \Psi_{eq}(r) + \tilde{\Psi}(r, \theta, z) - \frac{r^2}{2} \frac{n}{m} \frac{B_0}{R_0}. \quad (12)$$

The  $(m, n) = (1, 1)$  island is generated by the resistive interchange mode even  $\Psi_b = 0$ . This is due to the assumption of the large resistivity of  $S = 10^4$  and the cylindrical geometry. The X-point is generated at  $\theta = \pi$  in  $z = 0$  poloidal cross section in this case. Dashed line shows the position of the rational surface with  $\iota = 1$ . The vortex flow occurs so that the plasma inside  $\iota = 1$  surface moves toward the X-point.

Next, we consider the cases of the finite initial static islands. The dependence of  $w_s$  on  $w_i$  or  $\Psi_b$  is different between large and small cases of  $|w_i|$ .

In the large  $|w_i|$  case of  $|w_i| \geq 5.3 \times 10^{-2}$  ( $|\Psi_b| \geq 5.0 \times 10^{-4}$ ), there exists a tendency that  $|w_s|$  increases as  $|w_i|$  as shown in Fig.3.

Figure 6 shows the time evolution of the magnetic energy for  $w_i = 0.10$  ( $\Psi_b = 2.0 \times 10^{-3}$ ). As in the case of  $w_i = 0$ , there exists a stationary saturation state, however, the behavior of the mode in the linear region is different. Since  $\Psi_{1,1}$  has a large and constant amplitude due to static magnetic islands, the growth rate of  $\Psi_{1,1}$  is almost zero. The growth rates of other modes are determined by the convolution with  $\Psi_{1,1}$ , therefore, each mode has almost the same growth rate. This property of the linear growth rate is common for all finite  $w_i$ , but quite different from that in the case of  $w_i = 0$  shown in Fig.4.

In the initial state for  $w_i = 0.10$  ( $\Psi_b = 2.0 \times 10^{-3}$ ), the X-point is located at  $\theta = 0$  as shown in Fig.7(a). This point remains at the same position in the saturation state as shown in Fig.7(b). That is, the phase of the island in the saturation state is determined by that in the initial state, which is independent of the island phase of  $w_i = 0$ . In this case,  $|w_s|$  is smaller than  $|w_i|$  and the vortices are generated so that the plasma inside of the  $\iota = 1$  surface moves from the X-point to the O-point as shown in Fig.7. This result indicates that the interchange mode reduces the island width in the nonlinear evolution. This property is common for large initial island cases of  $|w_i| \geq 5.3 \times 10^{-2}$

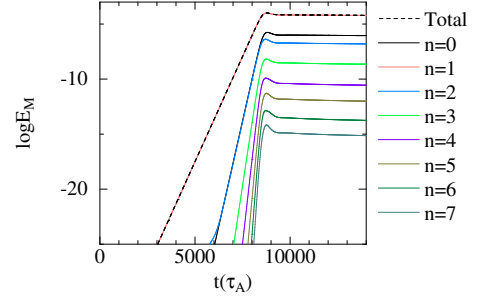


Fig. 4 Time evolution of the magnetic energy for  $w_i = 0$ .

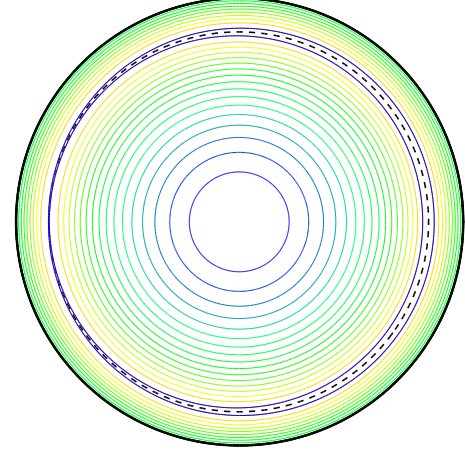


Fig. 5 Contour of helical magnetic flux in  $z = 0$  poloidal cross section at  $t = 14,000\tau_A$ .

( $|\Psi_b| \geq 5.0 \times 10^{-4}$ ).

On the other hand, in the small initial static island case of  $|w_i| < 5.3 \times 10^{-2}$  ( $|\Psi_b| < 5.0 \times 10^{-4}$ ), the dependence of  $w_s$  on  $w_i$  or  $\Psi_b$  is not monotonous, rather oscillatory, as shown in Fig.3. The property of the island development is different from that in the large initial island case.

Figure 8 shows the change of the magnetic islands for  $w_i = 4.1 \times 10^{-2}$  ( $\Psi_b = 3.0 \times 10^{-4}$ ). In this case, the phase of the islands are the same as that for  $|w_i| = 5.3 \times 10^{-2}$ , however,  $w_s$  is larger than  $w_i$  as shown in Fig.8(a) and (b). Figure 8(c) shows that the vortices are generated so that the plasma inside of the  $\iota = 1$  surface moves from the O-point to the X-point. This flow is considered to enhance the reconnection at the X-point. Therefore, the interchange

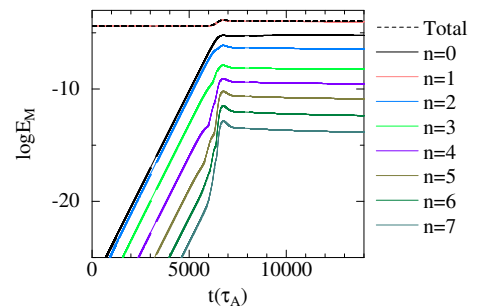


Fig. 6 Time evolution of magnetic energy .

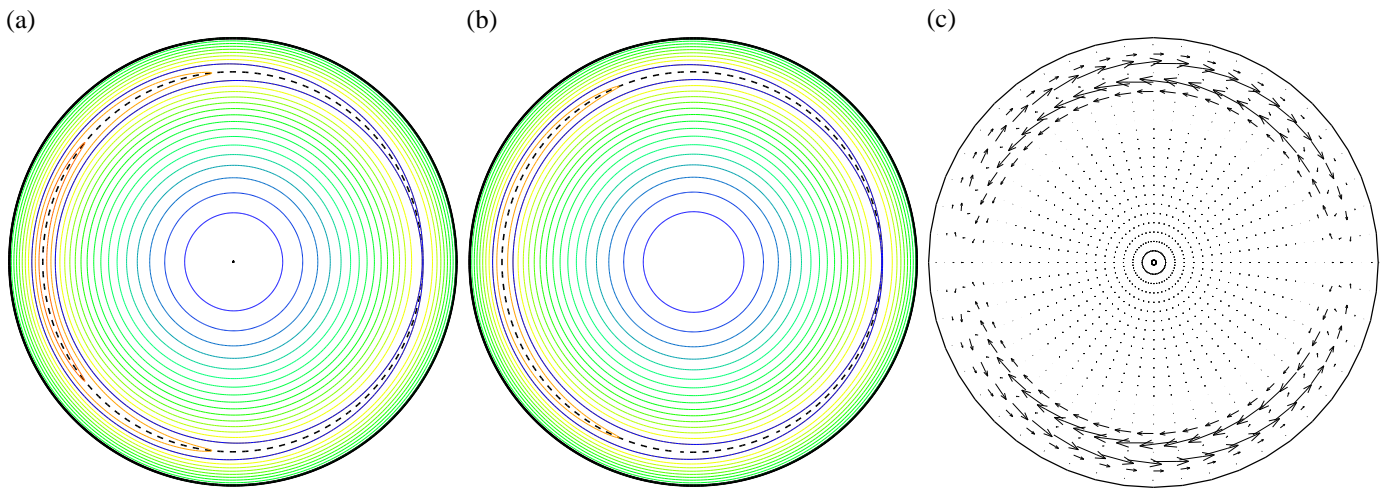


Fig.7 Contour of helical magnetic flux for  $w_i = 0.10$  at (a)  $t=0\tau_A$  and (b)  $t = 14,000\tau_A$ , and (c) flow pattern at  $t = 14,000\tau_A$  for the same  $w_i$ .

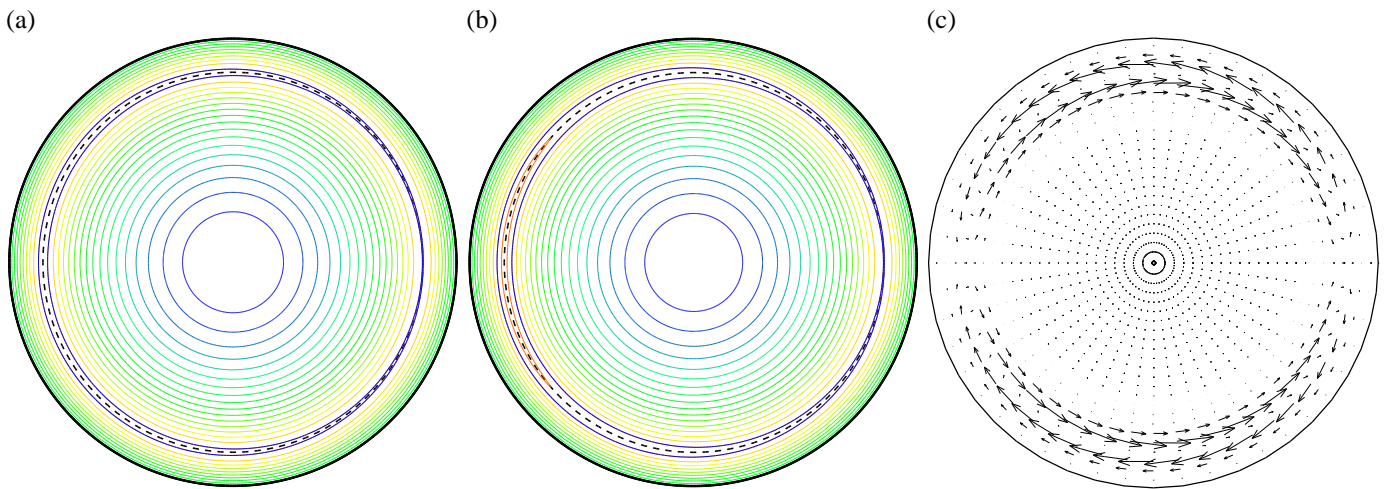


Fig.8 Contour of helical magnetic flux for  $w_i = 4.1 \times 10^{-2}$  at (a)  $t=0\tau_A$  and (b)  $t = 14,000\tau_A$ , and (c) flow pattern at  $t = 14,000\tau_A$  for the same  $w_i$ .

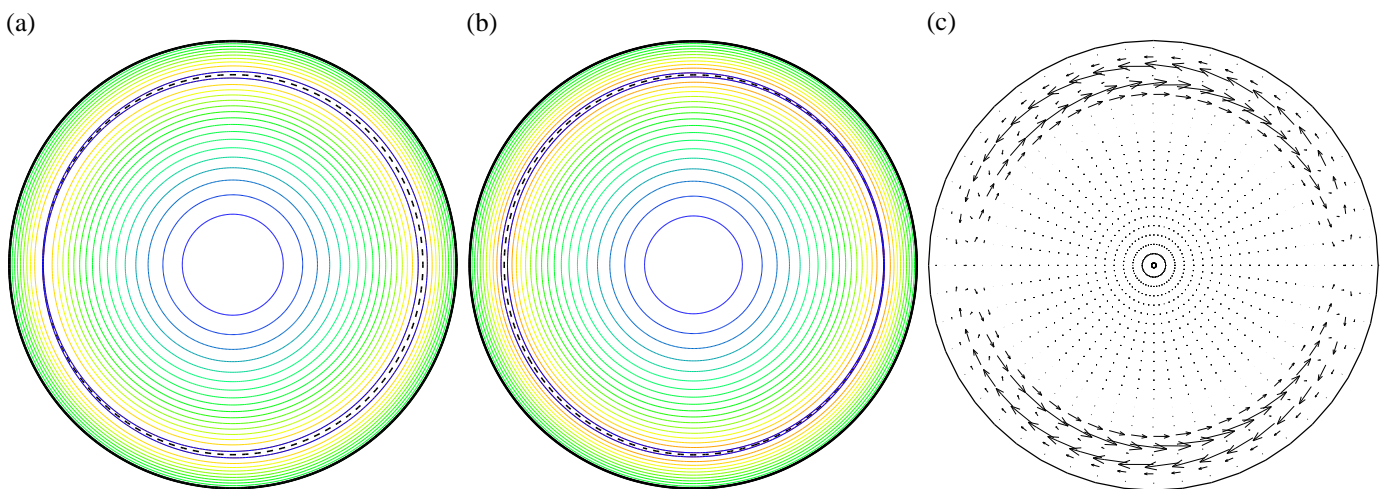


Fig.9 Contour of helical magnetic flux for  $w_i = -4.1 \times 10^{-2}$  at (a)  $t=0\tau_A$  and (b)  $t = 14,000\tau_A$ , and (c) flow pattern at  $t = 14,000\tau_A$  for the same  $w_i$ .

mode enhances the island width in the case.

In the case of  $w_i = -4.1 \times 10^{-2}$  ( $\Psi_b = -3.0 \times 10^{-4}$ ), we obtain another behavior of the island. In this case, the phase of the island changes in the nonlinear evolution of the interchange mode. The X-point is located at  $\theta = \pi$  at  $t = 0$ , while the point is located at  $\theta = 0$  at  $t = 14,000\tau_A$  as shown Fig. 9(a) and (b). The vortices are generated so that the plasma inside the  $\iota = 1$  surface moves from X-point to O-point in the initial island as shown in Fig. 9(c). The direction of the flow is the same as in the large initial island case, however, it may be strong enough to change the island phase.

## 5. Conclusions

We study the interaction between the  $(m, n) = (1, 1)$  static magnetic islands and the nonlinear dynamics of the resistive interchange mode with the single helicity of  $n/m = 1$  by following the time evolution of the mode. Particularly, the dependence of the island development on the width of the initial static island  $w_i$  is focused.

At first, we obtain a common feature in the linear state of the time evolution of the interchange mode for all finite  $w_i$ . The  $(m, n) = (1, 1)$  component of the magnetic energy is dominant and almost constant due to the existence of the initial state islands in the present analysis. Therefore, other components have almost the same growth rate because these components are mainly generated by the convolution with the dominant mode.

As the interchange mode evolves nonlinearly, the width and the phase of the magnetic islands can change. Such change are considered to be attributed to the vortex flow generated by the interchange mode. A common tendency between the flow and the change of the islands is also found for all finite  $w_i$ . When the flow is generated so that the plasma moves toward the initial O-point, the island width is reduced or the phase of the island is changed. On the other hand, the flow is generated so that the plasma moves toward the initial X-point, the island width is enhanced.

The dependence of the island width in the saturation state on  $w_i$  is different between the cases of the large and small  $|w_i|$ . In the large initial island case for  $|w_i| \geq 5.3 \times 10^{-2}$ , the island width in the saturation state increases monotonously as  $|w_i|$ . The location of the O-points and the X-points is determined by the positions in the initial islands and independent of the island phase for  $w_i = 0$ . In this case, the interchange mode has a contribution to reduce the island width for each  $w_i$ .

On the other hand, in the small island case for  $|w_i| < 5.3 \times 10^{-2}$ , the island development does not have such a definite tendency as in the large island case. The dependence of the island width in the saturation on  $w_i$  is not monotonous. In one case, the width is enhanced by the interchange mode evolution with the phase fixed. In other case, the island phase changes so that the positions of the X-point and the O-point are replaced in the saturation state.

Such behavior in the small island cases may be due to the existence of a large island for  $w_i = 0$ , which results from the choice of the large resistivity of  $S = 10^4$  in this analysis.

## Acknowledgments

This work is supported by NIFS cooperation programs NIFS08KLDD015 and NIFS08KNXN129 and by the Grant-in-Aid for Scientific Research (C) 17560736 of the Japan Society for the Promotion of Science.

## References

- [1]N. Ohyaabu et al., J. Nucl. Mater. **266-269** 302 (1999).
- [2]K. Ichiguchi et al., Nucl. Fusion **43**, 1101-1109 (2003).
- [3]T. Unemura et al., Phys. Plasmas **11** 1545 (2004).
- [4]S. P. Hirshman et al., Comput. Phys. Commun. **43** 143 (1986).